Centipedes subdue giant prey by blocking KCNQ channels

Lei Luo[a,b,c,1], Bowen Li[a,b,c,1], Sheng Wang[d,1], Fangming Wu[e,f,1], Xiaochen Wang[g,h], Ping Liang[g,h], Rose Ombati[a,b,c], Junji Chen[i], Xiancui Lu[a,b,c], Jianmin Cui[j,k], Qiumin Lu[a,b], Longhua Zhang[e,f], Ming Zhou[j,l,2], Changlin Tian[e,f,2], Shilong Yang[a,b,2], and Ren Lai[a,b,2]

[a]Key Laboratory of Animal Models and Human Disease Mechanisms of Chinese Academy of Sciences, Kunming Institute of Zoology, Kunming 650223, Yunnan, China; [b]Key Laboratory of Bioactive Peptides of Yunnan Province, Kunming Institute of Zoology, Kunming 650223, Yunnan, China; [c]University of Chinese Academy of Sciences, Beijing 100049, China; [d]Key Laboratory of Molecular Biophysics of the Ministry of Education College of Life Science and Technology, Huazhong University of Science and Technology, Wuhan, Hubei 430074, China; [e]Hefei National Laboratory of Physical Sciences at Microscale and School of Life Sciences, University of Science and Technology of China, Hefei 230027, China; [f]High Magnetic Field Laboratory, Chinese Academy of Sciences, Hefei 230027, China; [g]The First Affiliated Hospital, Zhejiang University School of Medicine, Hangzhou 310006, China; [h]Institute of Translational Medicine, Zhejiang University, Hangzhou 310058, China; [i]Chongzhou People's Hospital, Sichuan Academy of Medical Sciences, Chengdu 611230, China; [j]Ion Channel Research and Drug Development Center, Kunming Institute of Zoology, Chinese Academy of Sciences, Kunming 650223, China; [k]Department of Biomedical Engineering, Center for the Investigation of Membrane Excitability Diseases, Washington University in St Louis, St. Louis, MO 63130; and [l]Verna and Marrs McLean Department of Biochemistry and Molecular Biology, Baylor College of Medicine, Houston, TX 77030

Edited by Richard W. Aldrich, The University of Texas at Austin, Austin, TX, and approved December 13, 2017 (received for review August 22, 2017)

Centipedes can subdue giant prey by using venom, which is metabolically expensive to synthesize and thus used frugally through efficiently disrupting essential physiological systems. Here, we show that a centipede (*Scolopendra subspinipes mutilans*, ∼3 g) can subdue a mouse (∼45 g) within 30 seconds. We found that this observation is largely due to a peptide toxin in the venom, SsTx, and further established that SsTx blocks KCNQ potassium channels to exert the lethal toxicity. We also demonstrated that a KCNQ opener, retigabine, neutralizes the toxicity of a centipede's venom. The study indicates that centipedes' venom has evolved to simultaneously disrupt cardiovascular, respiratory, muscular, and nervous systems by targeting the broadly distributed KCNQ channels, thus providing a therapeutic strategy for centipede envenomation.

centipede | toxicity | SsTx | KCNQ

Predators usually catch prey that are smaller than themselves because capture success is a function of relative prey/predator size. It declines as the ratio increases (1, 2), but there is anecdotal evidence that centipedes subdue prey much larger than themselves by means of venoms (3, 4). Venomous predators use potent venom to immobilize large prey as well as defend against predators (5). However, venom is metabolically expensive to synthesize. For example, the metabolic rate of snakes increased by an average of 11% during a 3-d study over which venom regeneration was measured (6). Thus, venoms are used frugally by effectively targeting essential physiological systems, such as nervous, respiratory, circulatory, and muscular systems, to ensure successful capture of prey (2, 7).

Snake venoms target circulatory or nervous systems to effectively capture prey (7), while spiders, scorpions, and snails often immobilize prey by using venoms that act on the nervous system (8, 9). Although some insights may be gleaned from recent work on centipede toxins (10–13), the underlying mechanism of how centipedes capture giant prey remains unknown.

Centipede envenomations occur frequently. In Hawaii, centipede bites were responsible for 11% of the cases that presented to hospital emergency departments from 2007 to 2011 (14). Severe clinical symptoms, such as vasospasm, acute hypertension, myocardial ischemia, and even death, have been observed following centipede envenomation (15–18). These symptoms point to cardiovascular disorders, and based on our knowledge of scorpion and spider toxins, ion channels are the likely targets. We screened centipede venom against various ion channels and found that a peptide toxin, SsTx, is extremely potent on all members of the KCNQ family of potassium ion channels. KCNQ is a family of multifunctional K^+ channels that are involved in a diverse array of physiological functions, such as cardiac action potential repolarization, coronary circulation and reactive hyperemia, and cerebral neuron excitation (19, 20). KCNQ channels are also found in airway smooth muscle cells from rodent and human bronchioles (21). Based on the clinical symptoms caused by centipede bites and the role of KCNQ in essential physiological systems, we tested the following two hypotheses: (*i*) centipede venom blocks KCNQ channels to disrupt multiple essential physiological systems, such as cardiovascular, respiratory, and nervous systems, and thus (*ii*) KCNQ openers may neutralize toxicities caused by centipede envenomation.

Results

Centipedes Rapidly Subdue Mice. To test if centipedes are capable of rapidly subduing giant prey, golden head centipedes (*Scolopendra subspinipes mutilans*) with an individual body weight of ∼3 g were kept with a mouse (∼45 g) to observe their interactions. As illustrated in Fig. 1*A* and Movie S1, a single centipede immediately attacked the mouse and subdued it within 30 s. The LD_{50} values of the centipede crude venom in mice were 130 and 93 mg/kg after i.m. and i.p. injections, respectively (Fig. 1*B*, *Inset*). Capture of giant prey has been reported for social foragers such as ants (22), spiders (23), or pseudoscorpions (24), in which

Significance

The work showed that centipede venom can cause disorders in cardiovascular, respiratory, and nervous systems. The cardiovascular toxicity of the venom comes mostly from a peptide toxin SsTx, which blocks the KCNQ family of potassium channels. Retigabine, a KCNQ channel opener, neutralizes centipede venom toxicity, and thus could be used to treat centipede envenomation.

Author contributions: L.L., M.Z., C.T., S.Y., and R.L. designed research; L.L., B.L., X.L., and S.Y. performed research; S.W., F.W., X.W., P.L., J. Chen, L.Z., and C.T. contributed new reagents/analytic tools; L.L., B.L., X.W., P.L., and S.Y. analyzed data; and L.L., B.L., R.O., J. Cui, Q.L., M.Z., S.Y., and R.L. wrote the paper.

The authors declare no conflict of interest.

This article is a PNAS Direct Submission.

Data deposition: The NMR chemical shifts have been deposited in the Protein Data Bank, www.wwpdb.org (PDB ID code 5X0S), and GenBank database (accession no. MG585384).

[1]L.L., B.L., S.W., and F.W. contributed equally to this work.

[2]To whom correspondence may be addressed. Email: mzhou@bcm.edu, cltian@ustc.edu.cn, yangsl@mail.kiz.ac.cn, or rlai@mail.kiz.ac.cn.

This article contains supporting information online at www.pnas.org/lookup/suppl/doi:10.1073/pnas.1714760115/-/DCSupplemental.

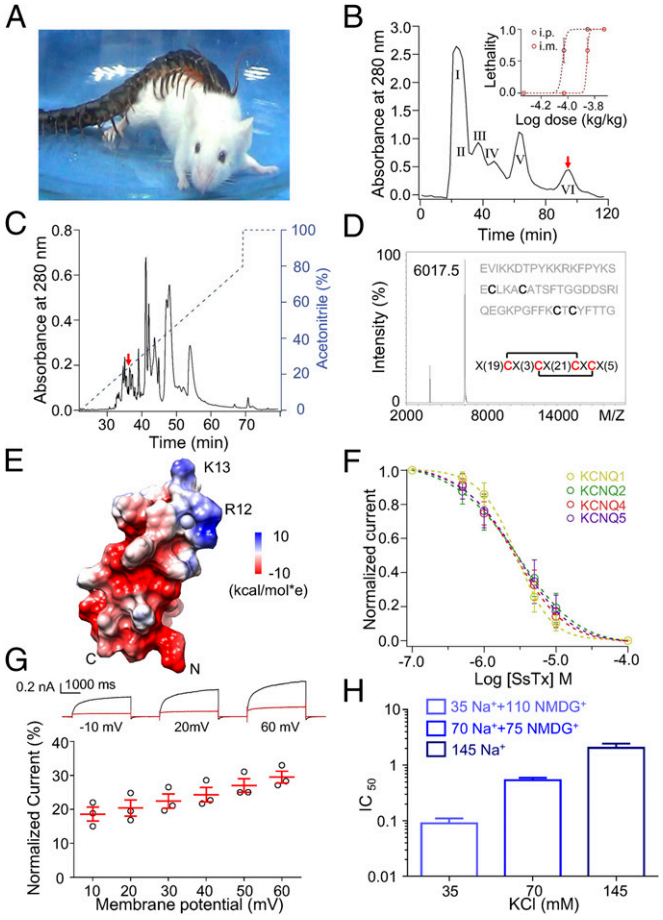

Fig. 1. Identification of a KCNQ blocker, SsTx, from the venom of *S. subspinipes mutilans*. (*A*) Image of a *S. subspinipes mutilans* preying on a Kunming mouse. (*B*) Diluted crude venom of golden head centipedes was subjected to Sephadex G-50 gel filtration. The protein fraction containing SsTx is marked as a red arrow. (*Inset*) Lethalty rate of mice recorded after i.p. and i.m. injection of crude venom and then fitted to a Hill equation (n = 3 animals per group, n = 3 groups per point). (*C*) Isolation of native SsTx (red arrow) from the pooled protein fraction by a C_{18} RP-HPLC column. (*D*) MALDI-TOF analysis and sequencing of SsTx, indicated by the 20-to-46 and 24-to-48 assignments. (*E*) NMR structural model of SsTx, with the electrostatic potential distribution shown in color (red = negative, blue = positive) on the right. The negatively charged surface and the location of R12 and K13 are shown on the NMR structure of SsTx. (*F*) Dose–response curves displaying the SsTx inhibition of KCNQ1, 2, 4, and 5. Data were fit with a Hill equation. The IC_{50} and slope factor values are 2.8 ± 0.5 μM and 1.74 ± 0.04 (n = 5 cells) for KCNQ1, 2.7 ± 0.4 μM and 0.99 ± 0.06 (n = 5 cells) for KCNQ2, 2.5 ± 0.4 μM and 1.18 ± 0.03 (n = 5 cells) for KCNQ4, and 2.7 ± 0.5 μM and 1.12 ± 0.06 (n = 5 cells) for KCNQ5, respectively. (*G*) The inhibitory percentage of KCNQ4 currents in the presence of 10 μM SsTx, recorded with increases in test pulses from a resting membrane potential of −80 mV (n = 3). (*H*) The half-maximum response of SsTx in different K^+ concentrations recorded from KCNQ4-expressing HEK293T cells (n = 5 cells per bar). Average values represent means ± SEMs.

the prey is subdued by several individuals. A single spider, *Zodarion cyrenaicum*, can capture a giant ant within 10–20 min (25). By contrast, the capture efficiency of the centipede is much higher than that of the spider. This is possible because the centipedes' venom has evolved to disrupt multiple essential physiological systems.

Isolation and Identification of KCNQ Inhibitor from Centipede Venom. We tracked the toxin that causes the lethal activity by using peptide purification coupled with toxicity experiments (Fig. 1 *B* and *C*). A small peptide toxin [named here Ssm Spooky Toxin (SsTx); GenBank accession no. MG585384], with a molecular weight of 6,017.5 Da, was subsequently identified from the centipede venom (Fig. 1*D*). The primary sequence of mature SsTx was obtained by Edman degradation (Fig. 1*D*), and the sequence shows no resemblance to any known animal toxins by a search of nonredundant protein databases, via the BLAST server (https://blast.ncbi.nlm.nih.gov/Blast.cgi). Comparing the purified SsTx with the premature one, we found that the 76-amino acid peptide undergoes posttranslational modification by cleaving off a signal peptide of 23 amino acids in length and yielding the mature peptide of 53 amino acids (Fig. S1*A*). Partial reduction and MS indicated that SsTx contains two intramolecular disulfide bridges: Cys20-Cys46 and Cys24-Cys48 (Fig. 1*D* and Fig. S1 *B–D*). SsTx structure was solved by solution NMR analysis (Fig. 1*E*, PDB 5X0S). The structure is compact, with amino acids in position 12 (arginine) and 13 (lysine), which form a positively charged surface (Fig. 1*E*). The C-terminal of the toxin is relatively flexible.

We examined SsTx on TRPV1, TRPV2, BK_{Ca}, hERG, voltage-gated sodium channels, voltage-gated potassium channels, and voltage-gated calcium channels (Fig. S1 *E–I* and *O*) and found that SsTx exhibits potent inhibitory effect on KCNQ4, with an IC_{50} of 2.5 ± 0.4 μM (Fig. S1 *J* and *K*). SsTx also inhibited other KCNQ channels with IC_{50} values of 2.8, 2.7, and 2.7 μM for the homotetrameric complexes of KCNQ1, KCNQ2, and KCNQ5, respectively (Fig. 1*F* and Fig. S1 *L–N*). Further analyses showed that SsTx blockade becomes progressively less when the membrane potential becomes more depolarized, and that higher K^+ concentrations increase the IC_{50} values (Fig. 1 *G* and *H*), consistent with a model in which SsTx binds to the outer pore domain of KCNQ channels (26). Since sequences of the outer pores of members of the KCNQ family exhibit high similarity, SsTx can inhibit different KCNQ channels and thus affect multiple physiological processes.

Direct Interaction Between SsTx and KCNQ Channels. Given that KCNQ4 is important in the regulation of pulmonary vascular tone, and blocking KCNQ4 increases the isometric tension of interlobular arteries (27), we hypothesized that SsTx may contribute to the vasospasm by inhibiting the KCNQ4 channel as reported in clinical cases of centipede envenomation (17). We therefore first investigated the interaction between SsTx and KCNQ4. The onset of channel inhibition upon perfusion of 10 μM SsTx is fast, with a time constant of 0.086 ± 0.011 s, and the recovery of channel current after washout of the toxin is relatively slow, with a time constant of 0.265 ± 0.007 s (Fig. S2 *A* and *B*), which is consistent with an IC_{50} of 2.5 μM. Alanine substitution was performed to identify residues important for SsTx's affinity on KCNQ4. Alanine substitution to six positively charged residues (K4A, K10A, K11A, R12A, K13A, and K45A) reduces the toxin's inhibitory effect on KCNQ4 (Fig. 2 *A* and *B*). These mutant toxins preserved WT-like structural features (Fig. S2*C*), suggesting that the reduced inhibition is caused by a direct interaction between SsTx and KCNQ4. In particular, alanine substitution at positions 12 and 13 increased IC_{50} values to 104.7 and 117.5 μM, respectively, while that of the WT is 2.5 μM (Fig. 2*C*). These two residues in combination with other positively charged amino acids in the N-terminus form a positively charged surface in SsTx (Fig. 1*E*). Collectively, we concluded that this positively charge surface constitutes the bioactive binding surface for SsTx to target KCNQ channels. Consistent with this conclusion, conservative replacement of lysine with arginine (K13R) or vice versa (R12K) has minimal influence on SsTx inhibition of KCNQ channels (Fig. S2*D*).

Next, we explored the toxin-binding sites on KCNQ channels. Since toxin binding is reduced under depolarizing membrane potentials and under higher intracellular K^+ concentration (Fig. 1 *G* and *H*), similar to the "knock off" effect reported by earlier

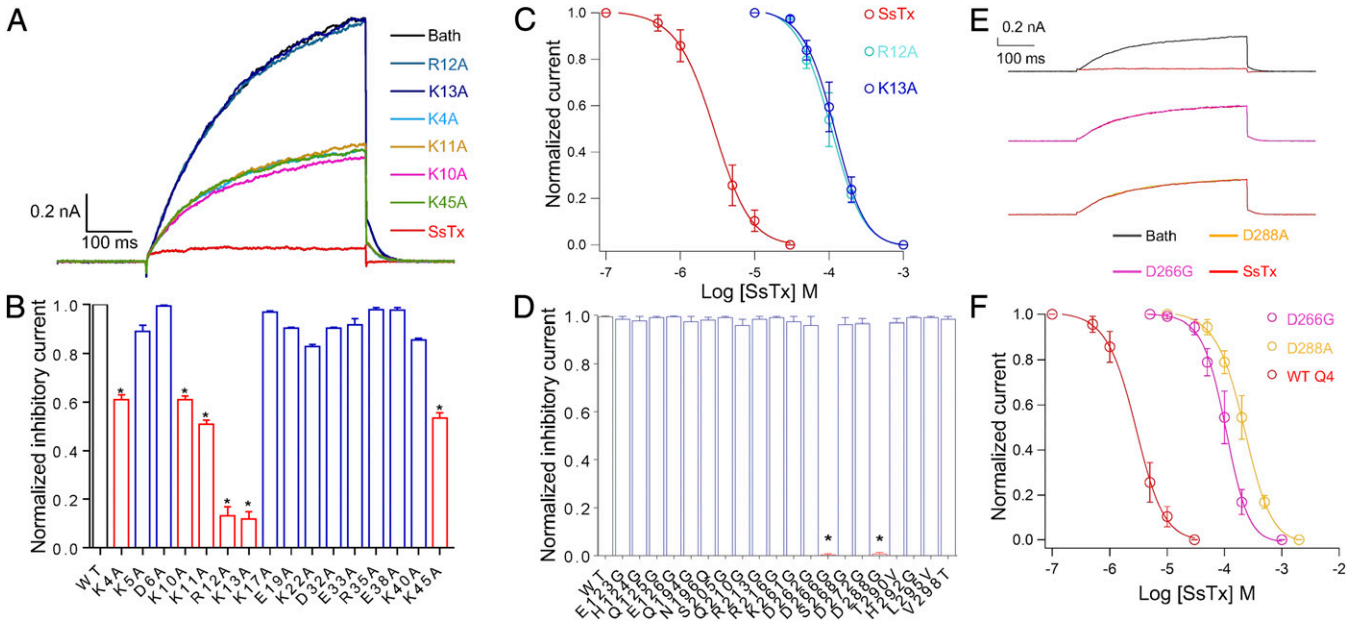

Fig. 2. Key residues involved in the interaction between SsTx and KCNQ4. (*A*) Representative whole-cell KCNQ4 currents from the same HEK293T cell recorded in the presence of 10 μM of WT SsTx and single point mutants (K4A, K10A, K11A, R12A, K13A, and K45A) sequentially. Before applications of each compound, the cells were perfused by bath solution for 30 s to ensure that the currents return to the same level. (*B*) Normalized inhibitory currents of 50 μM WT SsTx ($n = 3$) and 50-μM toxin mutants ($n = 10$). *$P < 0.05$ compared with WT group. (*C*) Inhibition of KCNQ4 by various concentrations of WT SsTx, R12A, and K13A. The data were fit to a Hill equation, and the IC_{50} and slope factor values are 2.5 ± 0.4 μM and 1.18 ± 0.05 ($n = 5$ cells) for WT SsTx, 104.7 ± 5.4 μM and 2.05 ± 0.09 ($n = 5$ cells) for R12A mutants, and 117.5 ± 6.1 μM and 1.93 ± 0.08 ($n = 5$ cells) for K13A mutants. (*D*) The normalized inhibitory currents of WT KCNQ4 ($n = 3$) and point mutants ($n = 5$) at extracellular domains in the presence of 31.6 μM SsTx. *$P < 0.05$ compared with the WT group. (*E*) Representative whole-cell WT KCNQ4 (*Top*), D266G (*Middle*), and D288A (*Bottom*) currents recorded in the presence of 10 μM SsTx. (*F*) Dose–response relationships of SsTx against WT KCNQ4, D266G, and D288A. Smooth curves are fit of data points to the Hill equation. The IC_{50} and slope factor values are 2.5 ± 0.4 μM and 1.18 ± 0.05 ($n = 5$ cells) for WT SsTx, 108.2 ± 6.3 μM and 2.11 ± 0.09 ($n = 5$ cells) for D266G mutants, and 218.8 ± 7.6 μM and 1.76 ± 0.08 ($n = 5$ cells) for D288A mutants. Average values represent means ± SEMs.

studies on charybdotoxin (26), we postulated that SsTx interacts with the pore domain of KCNQ channels. This hypothesis is consistent with SsTx's positively charged bioactive surface. We made point mutations to the residues located on the extracellular side outer-pore region as well as the extracellular loops of the KCNQ4 α subunit. We found that D266 in the turret and D288 in the P-loop region are crucial in SsTx-induced inhibition (Fig. 2*D*). In the presence of 10 μM SsTx, ∼99 and 97% inhibitory activity was lost in KCNQ4_D266G and KCNQ4_D288A, respectively (Fig. 2*E*). As illustrated in Fig. 2*F*, the IC_{50} of SsTx on WT KCNQ4 is 2.5 μM, and the value becomes 108.2 μM for KCNQ4_D266G and 218.8 μM for KCNQ4_D288A. In addition, mutations at both positions did not affect voltage activation of KCNQ4 (Fig. S2*E*), suggesting that these residues directly affect SsTx-KCNQ4 interaction. In a structural homology model of KCNQ4, D266 and D288 form a negatively charged surface near the outer-pore region that could interact with SsTx (Fig. S3*B*).

To further validate interactions between the positively charged residues on SsTx and the negatively charged residues of KCNQ4, we applied thermodynamic mutant cycle analysis (28–30) to experimentally investigate the molecular interactions between SsTx and KCNQ4 (Fig. 3*A*, *Top*). The interaction between the residue pair is considered energetically significant when the calculated interaction Ln(Ω) is much larger than the other pairs (31). As illustrated in Fig. 3 *A*–*D*, residue K13 from SsTx and D266 from KCNQ4 has an Ln(Ω) of 3.12, while the Ln(Ω) values are much smaller between residues K4, K10, K11, R12, or K45 on SsTx and residue D266 on KCNQ4. Similarly, residue R12 of SsTx and residue D288 of KCNQ4 has an Ln(Ω) value of 2.53, while the Ln(Ω) values for residues K4, K10, K11, K13, or K45 on SsTx and residue D288 on KCNQ4 are all much smaller (Fig. 3 *E* and *F* and Fig. S2*F*). These results indicate that residues R12 and K13 on SsTx functionally interact with residues D288 and D266 on KCNQ, respectively.

We would like to point out that Ln(Ω) values calculated based on IC_{50} measurements cannot be interpreted simply as a measure of physical interactions. In addition, the Hill slope is 1.18 ± 0.03 for inhibition of KCNQ4 by SsTx (Fig. 1*F*), and thus multiple SsTx molecules could interact with positive synergy to inhibit the channel. Consistent with this interpretation, docking of SsTx onto a structural model of KCNQ4 shows that multiple SsTx can be accommodated simultaneously (Fig. 3*E* and Fig. S2*G*). Regardless of these complications, D266 and D288 are highly conserved in all members of the KCNQ family (Fig. S2*H*) and thus could form the same "hot spots" in the pore region of all KCNQ channels. The negatively charged surface patch is also complementary to the positively charged surface on the toxin. Overall, our results indicate that the molecular interaction between SsTx and KCNQ channels is formed by at least two specific interacting residue pairs as well as van der Waals or electrostatic interactions contributed by K4, K10, K11, and K45.

SsTx Impairs Cardiovascular Systems. We subsequently investigated the in vivo effects of SsTx and centipede crude venom on cardiovascular systems. Following 5- and 10-mg/mL administration of the venom, the constriction force of the coronary artery increased by ∼1.6 (80%) and ∼2.1 (105%) g, respectively, compared with ∼2.2 g (110%) induced by the positive control, saturated phenylephrine (Fig. 4*A*). To determine if SsTx is the key component of the venom that causes vessel disorder, we compared the vessel activity of crude venom both in the presence and absence (CV-SsTx free or CV-Sf) of SsTx. As shown in Fig. 4*B*, CV-Sf (crude venom without SsTx) has only a small effect on arterial tension. Compared with 10 mg/mL crude venom-induced

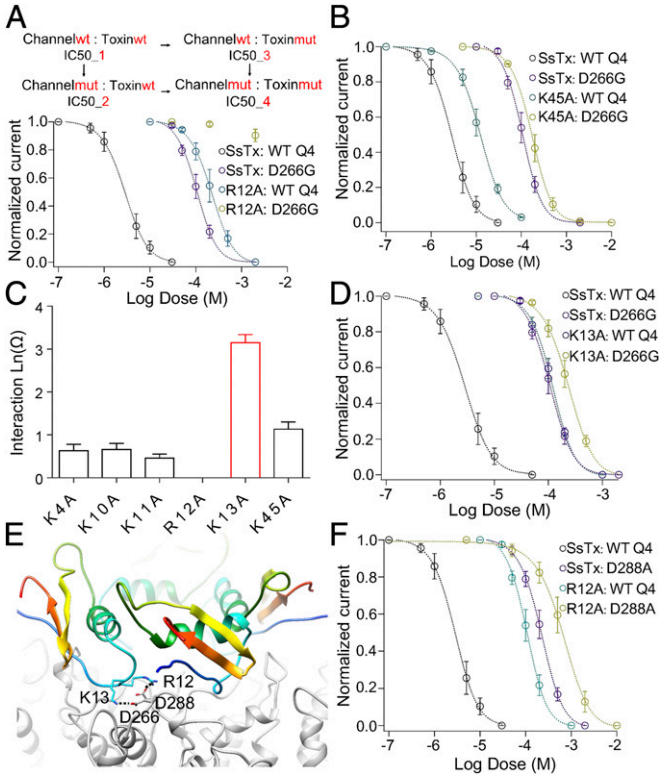

Fig. 3. Mutant cycle analysis for pairwise coupling of R12/D288 and K13/D266 (*A*, *Top*) schematic diagram of the mutant cycle analysis (*Top*; IC_{50}_1 indicates IC_{50} value measured from the condition where WT channels are inhibited by SsTx). (*A*, *Bottom*) Representative concentration–response curves for determining the interaction Ln(Ω) value between R12 and D266 [n = 10, SsTx (WT):KCNQ4(WT); n = 5, SsTx(WT):KCNQ4(D266G); n = 4, SsTx(R12A):KCNQ4(WT); n = 6, SsTx(R12A):KCNQ4(D266G)]. (*B*) Representative dose–response curves for the SsTx 45K and KCNQ4 D266 pair [n = 10, SsTx(WT):KCNQ4(WT); n = 5, SsTx(WT):KCNQ4(D266G); n = 5, SsTx(K45A):KCNQ4(WT); n = 6, SsTx(K45A):KCNQ4(D266G)]. (*C*) Summary of interaction Ln(Ω) values (n = 6 for K13/D266 pair, n = 3 for other pairs). (*D*) Dose–response curves for determining the interaction Ln(Ω) value between the SsTx K13 and KCNQ4 D266 pair [n = 10, SsTx(WT):KCNQ4(WT); n = 5, SsTx(WT):KCNQ4(D266G); n = 4, SsTx(K13A):KCNQ4(WT); n = 8, SsTx(K13A):KCNQ4(D266G)]. (*E*) Molecular docking of SsTx onto KCNQ4. The side chains of R12/K13 in SsTx and D266/D288 in KCNQ4 are shown. (*F*) Dose–response curves for determining the interaction Ln(Ω) value between the SsTx R12 and KCNQ4 D288 pair [n = 10, SsTx(WT):KCNQ4(WT); n = 5, SsTx(WT):KCNQ4(D288A); n = 4, SsTx (R12A):KCNQ4(WT); n = 6, SsTx(R12A):KCNQ4(D288A)]. mut, mutant.

vasoconstriction, which was ∼105%, 10 mg/mL CV-Sf only increases the vasoconstriction by ∼7.5%, indicating that SsTx is the main active component in the venom that exerts vessel activity. As expected, 1 and 5 μM SsTx increased the constriction force of the coronary artery by ∼50.3 and ∼105%, respectively (Fig. 4*C*). Consistent with the biological mechanism of SsTx, the vessel toxicity induced by centipede crude venom and SsTx was significantly reduced by retigabine (Fig. 4 *D* and *E*), a KCNQ opener (Fig. 4*F* and Fig. S3*A*).

As expected, both centipede crude venom and SsTx indeed exhibit potent activity of vasoconstriction in vivo (Fig. 5). Intravenous injection of crude venom induced acute hypertension in mice (Fig. 5*A*). Additionally, 0.5 mg/kg SsTx induced vasoconstriction, which further caused a significant increase in blood pressure (increased by 30.4 ± 5.7% in systolic blood pressure and by 40 ± 6.3% in diastolic blood pressure) in mice (Fig. 5*B*). SsTx also caused vasospasm and acute hypertension in *Macaca* monkeys while atropine and retigabine inhibited the effects (Fig. 5 *C* and *D*). Intravenous injection of retigabine (1 mg/kg) reversed hypertension induced by SsTx (0.1 mg/kg) as the blood pressure was reduced from ∼196 mmHg to a normal range (Fig. 5*D*). Following i.v. injection of SsTx, the mice kept twitching and shaking before death (Movie S2), yielding an LD_{50} of ∼0.85 mg/kg and the elimination half-life of 4.5 h (Fig. S6*C*). This lethal activity is likely due to coronary-induced myocardial ischemia, because we observed an inverted T wave in monkeys (Fig. 5*E*) after 5 min of i.v. injection of SsTx. The inverted T wave is a typical syndrome for myocardial ischemia (32). The inverted T wave was also reversed by retigabine (Fig. 5*E*). Thus, SsTx-induced coronary spasm plays a key role in myocardial ischemia, which usually progresses to heart failure if ischemic symptoms are prolonged (33). Unlike scorpion toxins that inhibit BK_{Ca} currents to induce vasospasm (34, 35), centipedes may use a different strategy by inhibiting KCNQ4 (Fig. S1*O*). We estimate that one bite from a centipede likely injects 15–30 μL crude venom, which has a concentration of ∼400 mg peptides per milliliter, is sufficient to subdue a small rodent (Movie S1). Although crude venoms from certain snakes and snails have higher lethal activity than that of centipedes (36, 37), it is not clear how much volume is injected in each attack.

SsTx Causes Disorders of Nervous and Respiratory Systems. Neuronal KCNQ channels (including KCNQ2, 3, and 5) are the molecular correlates of the M-current (19). The importance of M-channels is illustrated by the fact that a 25% decrease in M-current leads to neonatal epilepsy in humans (38) and that a disruption of *kcnq2* in mice is lethal (39). Since our study shows that SsTx acts as a potent inhibitor of KCNQ2, KCNQ3, and KCNQ5 (Fig. 1*F*), we would like to test whether SsTx could cause seizure or severe nervous disorder in small animals. Since SsTx does not cross the blood–brain barrier, the risk of seizure in human after envenomation is less of a concern. However, it could be relevant in small animals where a centipede bite could go through the skulls. After

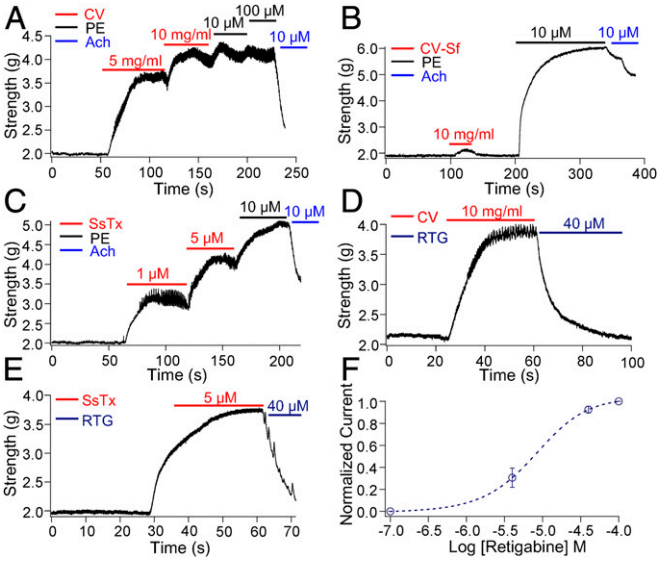

Fig. 4. Effects of SsTx on vascular contractility of thoracic aortas. Representative vascular contractility of thoracic aorta when challenged sequentially with (*A*) CV, PE, and ACh; (*B*) CV-Sf, PE, and ACh; (*C*) 1 and 5 μM SsTx, PE, and ACh; (*D*) 10 mg/mL CV and 40 μM RTG; and (*E*) 5 μM SsTx and 40 μM RTG. (*F*) Concentration–response curves of current increases at different concentrations of RTG in the presence of 5 μM SsTx. The smooth curve was a fitting of data points to the Hill equation. The average EC_{50} value is 7.83 ± 0.12 μM (n = 6 cells per data point). Increased currents from that in the presence of 5 μM SsTx were normalized by the increased currents in the presence of saturated RTG. CV, crude venom; PE, phenylephrine; RTG, retigabine.

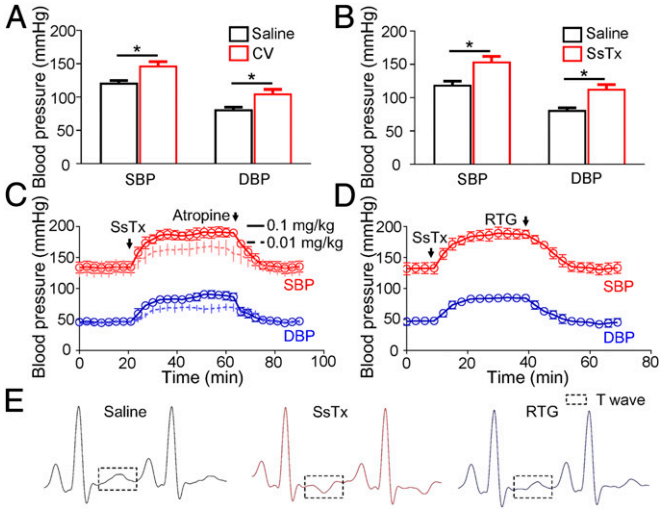

Fig. 5. SsTx causes disorders in the cardiovascular system. (*A*) Blood pressure of mice, including SBP and DBP recorded 10 min after i.v. injection of saline ($n = 6$ animals per bar) or CV (30 mg/kg, $n = 6$ animals per bar). *$P < 0.05$. (*B*) Blood pressure of mice, including SBP and DBP recorded 10 min after i.v. injection of saline ($n = 10$ animals per bar) or SsTx (0.5 mg/kg, $n = 10$ animals per bar). *$P < 0.05$. (*C*) Blood pressure of monkeys, including SBP (in red) and DBP (in blue) recorded every 3 min before and after i.v. injection of SsTx ($n = 3$, 0.1 mg/kg, solid line; $n = 3$, 0.01 mg/kg, dotted line) and atropine. (*D*) Blood pressure of monkeys, including SBP (in red) and DBP (in blue) recorded every 3 min before and after i.v. injection of SsTx ($n = 3$, 0.1 mg/kg; solid line) and RTG (1 mg/kg). (*E*) Representative three-lead surface ECG of a monkey recorded 10 min after i.v. injection of saline ($n = 3$) or SsTx ($n = 3$, 0.01 mg/kg) and followed by a rescue with RTG (1 mg/kg) after SsTx (0.01 mg/kg) injection ($n = 3$). CV, crude venom; DBP, diastolic blood pressure; RTG, retigabine; SBP, systolic blood pressure.

the injection of 1 μL of 20 μM SsTx in the hippocampus, mice developed seizures instantaneously (Movie S3), resulting in death after 10–20 min. Since M-current is important for action potential generation (39) and the release of neurotransmitter (40), the direct M-channel blockers are severely neurotoxic. To better understand the electrophysiological changes in hippocampal neurons after SsTx application, we conducted patch clamp recordings on brain slices of mice. At the concentration of 10 μM, SsTx evoked a spiking frequency of ∼20 Hz, much higher than the untreated neurons (∼12 Hz) (Fig. 6 *A* and *B*). Acetylcholine concentration in mice hippocampi increased by ∼63.6 and ∼81.8% after the administration of 1 μL of 10 μM SsTx and 100 μM linopirdine (a well-known inhibitor of KCNQ channels), respectively (Fig. 6*C*). As expected, retigabine inhibited the SsTx-induced increase in spiking frequency and acetylcholine secretion (Fig. 6 *A*–*C*), as well as seizure in mice (Movie S3).

Given KCNQ's important function in the respiratory system (21), effects of the crude venom and SsTx on rat respiratory functions were subsequently investigated (Fig. 6 *D*–*H*). Following the i.v. injection of SsTx, the respiratory rate was significantly decreased while respiratory amplitude was increased. One-and-one-half hours after administration of 2 mg/kg SsTx, the respiratory rate was reduced by ∼75% and respiratory amplitude increased by ∼150% (Fig. 6 *D*–*F*). In vitro experiments showed that crude venom (Fig. 6*G*) or SsTx (Fig. 6*H*) can induce bronchial ring contraction and that the contraction can be reduced by retigabine. Our results show that SsTx and the crude venom cause disorders not only on the cardiovascular system but also on nervous and respiratory systems.

Discussion

Although venom is a potent weapon for prey capture, its regeneration requires an increased metabolic rate over a long duration. Thus, strategies of venom optimization likely have evolved to minimize venom expenditure by venomous animals (7). Targeting of multiple essential physiological systems by centipede venom is an example of such venom optimization. The centipede toxin SsTx simultaneously disrupts several essential systems, including respiratory, cardiovascular, and perhaps the muscular system, by blocking multifunctional KCNQ channels. SsTx causes cardiovascular toxic symptoms including hypertension, myocardial

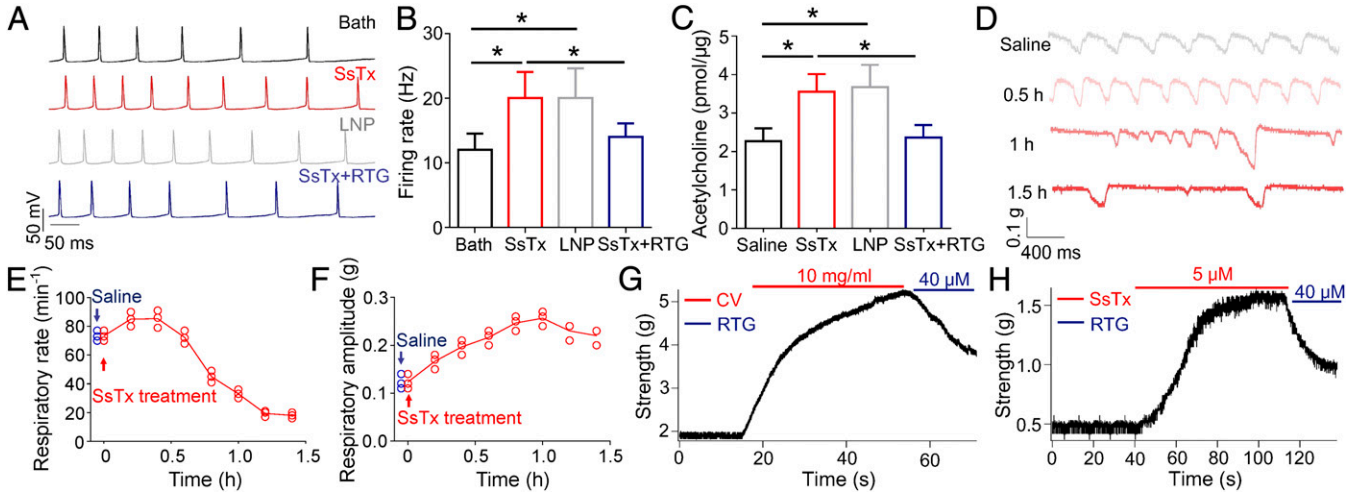

Fig. 6. SsTx interrupts nervous and respiratory systems. (*A*) Response of CA1 pyramidal neurons after application of 40 pA depolarizing current injected into the cell when challenged sequentially with 10 μM SsTx, 100 μM LNP, and the mixture of 10 μM SsTx and 40 μM RTG. Before applications of each compound, the brain slices were perfused by bath solution for 10 min to ensure that the firing rates return to the level before compound administration. (*B*) Summary of spiking frequency in the presence of bath solution ($n = 7$), 10 μM SsTx ($n = 7$), 100 μM LNP ($n = 7$), and the mixture of 10 μM SsTx and 40 μM RTG ($n = 4$). *$P <$ 0.05. (*C*) Acetylcholine concentrations quantified 30 min after microinjection of 1 μL of saline ($n = 6$), 20 μM SsTx ($n = 6$), 100 μM LNP ($n = 6$), or the mixture of 10 μM SsTx and 40 μM RTG ($n = 3$) into the hippocampus of mice. *$P < 0.05$. (*D*) Representative respiratory traces on rats were recorded before and after 2 mg/kg SsTx administration by i.v. injection. The changes in rats' respiratory rates (*E*) and amplitudes (*F*) when challenged with i.v.-injected SsTx ($n = 3$ animals per point, 2 mg/kg). Representative vascular contractility of bronchial ring contraction when challenged sequentially with (*G*) CV and RTG ($n = 3$ rats) and (*H*) SsTx and RTG ($n = 3$ rats). CV, crude venom; LNP, linopirdine; RTG, retigabine.

ischemia, vasospasm, and twitching (Figs. 4 and 5); neurotoxic symptoms such as seizure (Fig. 6 *A* and *B*); and respiratory disorders such as lowered respiratory rate (Fig. 6 *D* and *E*). These symptoms are clinically relevant because they have been observed in patients following centipede envenomation (17, 41). Removing SsTx from the crude venom significantly decreased the toxicity on the cardiovascular system (Fig. 4 *A* and *B*), demonstrating that the single venom component SsTx plays a crucial role in the prey–capture strategy.

Among case reports, tissue necrosis is a very common symptom caused by centipede envenomation. Indeed, local injection of SsTx in the back skin of mice caused significant tissue necrosis (Fig. S5). This local effect of SsTx is likely caused by spasm of capillary vessels. In comparison with other reported centipede crude venom activities, such as platelet-aggregating and phospholipase A2 activities (42), SsTx also seems to be a predominant factor for local symptoms, especially tissue necrosis.

Severe clinical cardiovascular symptoms, even death, have been reported following centipede bites, yet no effective therapeutic interventions are available. In this study, we illustrate that KCNQ channels are the likely targets for centipede venom and that the KCNQ opener retigabine, which is approved for treating epilepsy, could be used to treat centipede envenomation. Our experiments at the molecular, cellular, organ, and animal levels showed that retigabine reverses the effect of either crude centipede venom or purified SsTx. In conclusion, our work reveals that the centipede has evolved a simple yet powerful strategy to disable multiple essential physiological systems in prey and shows that an equally simple strategy could be effective in neutralizing the venom's toxicity.

Materials and Methods

Animal procedures were performed in compliance with the Institutional Animal Care and Use Committee of Laboratory Animals of Kunming Institute of Zoology, Chinese Academy of Sciences. For the video recording of the centipede's bite, the mice were put into a 2-L conical flask to adapt to the environment. The centipede was delivered into the conical flask after the mice were stabilized. Purification, NMR, tissue isolation, cell culture, and electrophysiological measurements were performed by using standard approaches. See *SI Materials and Methods* for a detailed description.

ACKNOWLEDGMENTS. We thank Prof. Kewei Wang for providing hKCNQ1, 2, and 4 plasmids; Prof. Hailin Zhang for providing hKCNQ 3 and 5 plasmids; Prof. Jiuping Ding for mBK_{Ca} and hβ1; Dr. NingNing Wei for gating kinetics analysis; and Dr. Shaoxing Dai for the convenient Discovery studio software installation. We also thank Lin Zeng for her work on SsTx disulfide bond parsing. We thank our laboratory members Zhanserik Shynykul, Yalan Han, Canwei Du, Xin Wang, and Yunfei Wang for discussion. This work was supported by funding from Ministry of Science and Technology of China Grant (2013CB911304), the National Science Foundation (NSF) of China Grants (331372208 and U1302221), the Chinese Academy of Sciences Grants (XDA12040209 and QYZDJ-SSW-SMC012), and Yunnan Province Grant (2015HA023; to R.L.), the NSF of China Grants (31640071 and 3177040928) and the Chinese Academy of Sciences Grants (XDA12020334 and Youth Innovation Promotion Association; to S.Y.), Yunnan Province Grant (2016FA006; to Q.L.), and the NSF of China Grant (31470740; to F.W.).

1. Balgooyen TC (1976) Behaviour and ecology of the American kestrel (Falco sparverius L.) in the Sierra Nevada of California. *Univ Calif Publ Zool* 103:1–84.
2. Griffiths D (1980) Foraging costs and relative prey size. *Am Nat* 116:743–752.
3. Dufton MJ (1992) Venomous mammals. *Pharmacol Ther* 53:199–215.
4. Undheim EAB, King GF (2011) On the venom system of centipedes (Chilopoda), a neglected group of venomous animals. *Toxicon* 57:512–524.
5. McCue MD (2005) Enzyme activities and biological functions of snake venoms. *Appl Herpetol* 2:109–123.
6. McCue MD (2006) Cost of producing venom in three North American pitviper species. *Copeia* 4:818–825.
7. Morgenstern D, King GF (2013) The venom optimization hypothesis revisited. *Toxicon* 63:120–128.
8. King GF, Hardy MC (2013) Spider-venom peptides: Structure, pharmacology, and potential for control of insect pests. *Annu Rev Entomol* 58:475–496.
9. Olivera BM, Seger J, Horvath MP, Fedosov AE (2015) Prey-capture strategies of fish-hunting cone snails: Behavior, neurobiology and evolution. *Brain Behav Evol* 86: 58–74.
10. Hakim MA, Yang S, Lai R (2015) Centipede venoms and their components: Resources for potential therapeutic applications. *Toxins (Basel)* 7:4832–4851.
11. Yang S, et al. (2012) Chemical punch packed in venoms makes centipedes excellent predators. *Mol Cell Proteomics* 11:640–650.
12. Yang S, et al. (2015) A pain-inducing centipede toxin targets the heat activation machinery of nociceptor TRPV1. *Nat Commun* 6:8297.
13. Undheim EA, et al. (2014) Clawing through evolution: Toxin diversification and convergence in the ancient lineage Chilopoda (centipedes). *Mol Biol Evol* 31: 2124–2148.
14. Guerrero AP (2007) Centipede bites in Hawai'i: A brief case report and review of the literature. *Hawaii Med J* 66:125–127.
15. Harada K, Asa K, Imachi T, Yamaguchi Y, Yoshida K (1999) Centipede inflicted postmortem injury. *J Forensic Sci* 44:849–850.
16. Logan JL, Ogden DA (1985) Rhabdomyolysis and acute renal failure following the bite of the giant desert centipede Scolopendra heros. *West J Med* 142:549–550.
17. Ozsarac M, Karcioglu O, Ayrik C, Somuncu F, Gumrukcu S (2004) Acute coronary ischemia following centipede envenomation: Case report and review of the literature. *Wilderness Environ Med* 15:109–112.
18. Yildiz A, et al. (2006) Acute myocardial infarction in a young man caused by centipede sting. *Emerg Med J* 23:e30.
19. Delmas P, Brown DA (2005) Pathways modulating neural KCNQ/M (Kv7) potassium channels. *Nat Rev Neurosci* 6:850–862.
20. Jentsch TJ (2000) Neuronal KCNQ potassium channels: Physiology and role in disease. *Nat Rev Neurosci* 1:21–30.
21. Brueggemann LI, et al. (2014) KCNQ (Kv7) potassium channel activators as bronchodilators: Combination with a β2-adrenergic agonist enhances relaxation of rat airways. *Am J Physiol Lung Cell Mol Physiol* 306:L476–L486.
22. Dejean A, et al. (2010) Arboreal ants use the "Velcro(R) principle" to capture very large prey. *PLoS One* 5:e11331.
23. Yip EC, Powers KS, Avilés L (2008) Cooperative capture of large prey solves scaling challenge faced by spider societies. *Proc Natl Acad Sci USA* 105:11818–11822.
24. Zeh JA, Zeh DW (1990) Cooperative foraging for large prey by Paratemnus-Elongatus (Pseudoscorpionida, Atemnidae). *J Arachnol* 18:307–311.
25. Pekár S, Šedo O, Líznarová E, Korenko S, Zdráhal Z (2014) David and Goliath: Potent venom of an ant-eating spider (Araneae) enables capture of a giant prey. *Naturwissenschaften* 101:533–540.
26. MacKinnon R, Miller C (1988) Mechanism of charybdotoxin block of the high-conductance, Ca2+-activated K+ channel. *J Gen Physiol* 91:335–349.
27. Stott JB, Barrese V, Jepps TA, Leighton EV, Greenwood IA (2015) Contribution of Kv7 channels to natriuretic peptide mediated vasodilation in normal and hypertensive rats. *Hypertension* 65:676–682.
28. Hidalgo P, MacKinnon R (1995) Revealing the architecture of a K+ channel pore through mutant cycles with a peptide inhibitor. *Science* 268:307–310.
29. Horovitz A, Fersht AR (1990) Strategy for analysing the co-operativity of intramolecular interactions in peptides and proteins. *J Mol Biol* 214:613–617.
30. Ranganathan R, Lewis JH, MacKinnon R (1996) Spatial localization of the K+ channel selectivity filter by mutant cycle-based structure analysis. *Neuron* 16:131–139.
31. Schreiber G, Fersht AR (1995) Energetics of protein-protein interactions: Analysis of the barnase-barstar interface by single mutations and double mutant cycles. *J Mol Biol* 248:478–486.
32. Moukarbel GV, Weinrauch LA (2012) Disruption of coronary vasomotor function: The coronary spasm syndrome. *Cardiovasc Ther* 30:e66–e73.
33. Ferrari R, et al. (1998) Metabolic derangement in ischemic heart disease and its therapeutic control. *Am J Cardiol* 82:2K–13K.
34. Crest M, et al. (1992) Kaliotoxin, a novel peptidyl inhibitor of neuronal BK-type Ca(2+)-activated K+ channels characterized from Androctonus mauretanicus mauretanicus venom. *J Biol Chem* 267:1640–1647.
35. Yao J, et al. (2005) BmP09, a "long chain" scorpion peptide blocker of BK channels. *J Biol Chem* 280:14819–14828.
36. Tan KY, Tan CH, Fung SY, Tan NH (2015) Venomics, lethality and neutralization of Naja kaouthia (monocled cobra) venoms from three different geographical regions of Southeast Asia. *J Proteomics* 120:105–125.
37. Saminathan R, et al. (2006) Clinico-toxinological characterization of the acute effects of the venom of the marine snail, Conus loroisii. *Acta Trop* 97:75–87.
38. Lerche H, Jurkat-Rott K, Lehmann-Horn F (2001) Ion channels and epilepsy. *Am J Med Genet* 106:146–159.
39. Watanabe H, et al. (2000) Disruption of the epilepsy KCNQ2 gene results in neural hyperexcitability. *J Neurochem* 75:28–33.
40. Eid CN, Jr, Rose GM (1999) Cognition enhancement strategies by ion channel modulation of neurotransmission. *Curr Pharm Des* 5:345–361.
41. Senthilkumaran S, Meenakshisundaram R, Michaels AD, Suresh P, Thirumalaikolundusubramanian P (2011) Acute ST-segment elevation myocardial infarction from a centipede bite. *J Cardiovasc Dis Res* 2:244–246.
42. Liu ZC, et al. (2012) Venomic and transcriptomic analysis of centipede Scolopendra subspinipes dehaani. *J Proteome Res* 11:6197–6212.